Mesostructured Fe Oxide Synthesized by Ligand-Assisted Templating with a Chelating Triol Surfactant

Andrei Lezau,[†] Michel Trudeau,[‡] Georgi M. Tsoi,[§] Lowell E. Wenger,[§,||] and David Antonelli*[,†]

Department of Chemistry and Biochemistry, The University of Windsor, 401 Sunset Avenue, Windsor, Ontario, Canada N9B-3P4, Emerging Technologies, Hydro-Québec Research Institute, 1800 Boul. Lionel-Boulet, Varennes, Quebec, Canada J3X 1S1, Department of Physics and Astronomy, Wayne State University, Detroit, Michigan 48201, and Department of Physics, The University of Alabama at Birmingham, Birmingham, Alabama 35294

Received: November 20, 2003; In Final Form: January 20, 2004

The synthesis and properties of sulfate- and phosphate-free mesostructured iron oxide prepared using a chelating triol surfactant are reported. Materials synthesized using metal−surfactant ratios of 1:1, 2:1, 3:1, and 4:1 all showed a broad single reflection in the XRD at low angle corresponding to a wormhole mesostructure, as well as small higher angle peaks consistent with the presence of a small amount of maghemite and hemitite. TEM images confirmed the wormhole structure of the mesophase, while also revealing rodlike crystals corresponding to one or both of the two known phases of iron oxide observed in the XRD. Attempts to remove the surfactant by washing or chemical treatment were unsuccessful. Calcination led to a complete collapse of the structure and crystallization of the mesophase into maghemite. Magnetic studies provided evidence for the formation of superparamagnetic iron oxide particles within the walls of the mesostructure in addition to a small magnetic contribution arising from the presence of larger maghemite crystallites, while the calcined materials behaved more like a soft ferromagnet.

Introduction

The synthesis of surfactant templated mesoporous inorganic oxides has been one of the most active areas of materials science since Mobil discovered MCM-41 in the early 1990s.[1,2] By controlling the pore size and pore channel architecture of silica via an appropriate choice of templates,[3−12] it is possible to synthesize materials with potential applications in the areas of catalysis,[13] sensors,[14] and optics[15] and in the fabrication of nanostructured electronic[16] or magnetic devices.[17] To further expand the properties of these porous architectures, several groups have synthesized mesoporous silicas with organic groups in the walls that can be readily altered to tailor the reactivity and properties of the pore channels.[18,19] Mesoporous materials can also be fabricated from a more catalytically and electrochemically active inorganic substance than silica, such as a transition-metal oxide[20−26] or sulfide.[27−29] One of the most interesting materials from the standpoint of solid ion batteries and magnetic properties is iron(III) oxide. While hexagonal and mesolammelar iron oxides and oxyhydroxides have been synthesized with phosphate[30] and sulfate surfactants,[31,32] there is as yet no report of an ordered mesostructured iron oxide without sulfate or phosphate in the walls, although Gedanken has synthesized an amorphous mesoporous iron oxide with surface areas of up to 270 m^2/g using a cationic alkylammonium surfactant.[33] Since ligand-assisted templating has proven to be an effective route into the synthesis of numerous mesoporous transition-metal oxides,[13] and iron(III) prefers coordination to tris-chelating hard oxygen donors, a chelating triol surfactant should be an ideal templating agent for the synthesis of mesoporous iron oxides. In previous work, we showed that mesostructured zirconias could be synthesized from 1,1,1- trishydroxymethylundecane and that the template could be removed by calcination without significant loss of the periodic pore structure.[34] This surfactant has a large headgroup volume, ideal for formation of tubular micelles, as opposed to layered phases as is often found with phosphate and acetate surfactants, and three hydroxyl groups, which are ideally situated to form a tris-chelating interaction with a metal center. Herein, we report the synthesis and magnetic properties of a new series of surfactant templated mesostructured iron oxides with no phosphate or sulfate in the walls.

Experimental Section

Materials and Equipment. All chemicals unless otherwise stated were obtained from Aldrich. Iron(III) ethoxide was obtained from Fluorochem. 1,1,1-trishydroxymethylundecane was synthesized by the literature method[35] and purified by recrystallization from chloroform and pentane. Nitrogen adsorption data was collected on a Micromeritics ASAP 2010. X-ray diffraction (XRD) patterns (CuKα) were recorded in a sealed glass capillary on a Seimens D-500 $\theta\angle 2\theta$ diffractometer. All X-ray photoelectron spectroscopy (XPS) peaks were referenced to the carbon C−(C,H) peak at 284.8 eV and the data were obtained using a Physical Electronics model PHI-5500 system using charge neutralization. TEM samples were prepared by sonication in 2-propanol followed by deposition on a silica-coated copper grid. Images were obtained on a Hitachi model H-9000 TEM at 300 kV. Magnetic measurements were conducted on a Quantum Design model MPMS-5S SQUID magnetometer system with a 5 T magnet. All elemental analysis data (conducted under an inert atmosphere) were obtained from

* Address correspondence to this author. E-mail: danton@uwindsor.ca.
[†] The University of Windsor.
[‡] Emerging Technologies.
[§] Wayne State University.
[||] The University of Alabama at Birmingham.

10.1021/jp031259h CCC: $27.50 © 2004 American Chemical Society
Published on Web 04/02/2004

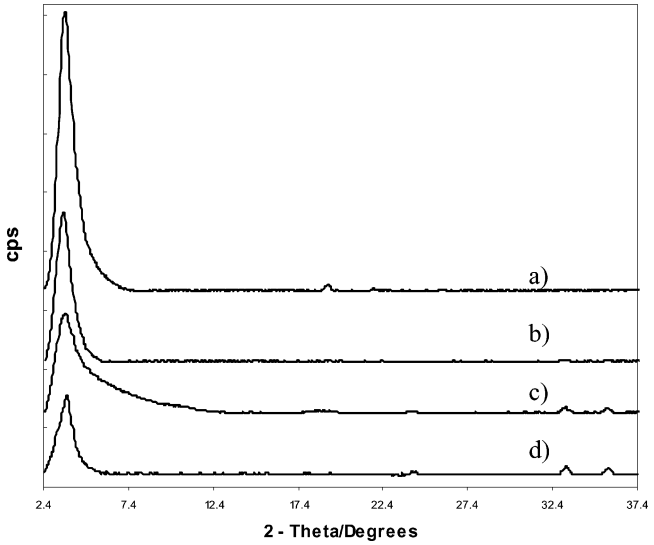

Figure 1. XRD patterns of mesostructured iron oxides synthesized at (a) 1:1, (b) 2:1, (c) 3:1, and (d) 4:1 metal-to-surfactant ratios.

Galbraith Laboratories (2323 Sycamore Drive, Knoxville, TN 37921-1700).

Synthesis. In a typical preparation, 2.091 g of iron ethoxide (0.0109 mol) were heated in 10 mL dry ethanol with 1.00 g 1,1,1-trishydroxymethylundecane (0.0036 mol). An equal volume of water was then added, forcing immediate precipitation of a heavy red solid. The mixture was left overnight and then transferred to an oven for aging at 60 °C for 2 days followed by 90 °C for 7 days. The solid was then collected by filtration and left in an oven at 110 °C for 5 days. Calcination was carried out at 400 °C for 4−8 h in air with a heating rate of 1 °C/min.

Results and Discussion

The X-ray powder diffraction (XRD) patterns for materials synthesized with $Fe(OEt)_3$-to-1,1,1-trishydroxymethylundecane ratios of 1:1, 2:1, 3:1, and 4:1 are shown in Figure 1. The materials all display a large central reflection corresponding to a repeat distance of 28 Å. The absence of any other low angle peaks indicates that this material possesses a wormhole mesostructure with no long-range mesoscopic order. There is no evidence of a layered mesophase, as is often observed in surfactant templated inorganic oxides at surfactant-to-inorganic ratios near 1:1. This may be attributable to the large headgroup volume of the surfactant which tends to favor cylindrical packing.[36] The other smaller reflections at higher angle, particularly evident in the 3:1 and 4:1 materials, can be indexed to a mixture of maghemite and hematite, which have previously been reported in synthesis mixtures of mesostructured iron oxides.[33] The overlapping reflections of these two phases make it difficult to determine their relative proportions. The presence of dense iron oxide phases indicates that the template-to-precursor interaction is not strong enough to prevent formation of template-free inorganic particles. The formation of varying amounts of template-free silica particles in MCM-41 synthesis mixtures is well documented; however, ligand-assisted templating with Zr, Nb, Ti, and Ta oxide precursors normally suppresses the formation of amorphous oxides by tethering the precursor strongly enough to the template to ensure that the vast majority of the metal ends up in the mesostructure and not a second template-free phase.[37] Elemental analysis of these materials show a steady increase in C and H content from 26.34% C and 4.46% H in the 4:1 material, 32.17% C and 5.63% H in the 3:1 material, 38.96% C and 6.65% H in the 2:1 material, and 49.55% C and 8.45% H in the 1:1 material. Transmission electron microscope (TEM) micrographs of all materials show the coexistence of a wormhole phase with rodlike nanocrystalline grains of a dense phase, consistent with the presence of maghemite and hematite in the XRD. The TEM micrograph of the 3:1 material, shown in Figure 2a with an expanded region shown in 2b, clearly reveals the wormhole structure with 18 Å pores and 10 Å walls, which is consistent with the XRD repeat distance of 28 Å. The rodlike crystals confirm that the additional XRD peaks at higher angle are a separate phase and are not due to crystallization of the walls of the mesostructure. The materials synthesized at different ratios provide similar TEM micrographs, containing a mixture of wormhole regions and discrete rodlike crystals. The X-ray photoelectron spectrum (XPS) of the 3p region of the 3:1 material is shown in Figure 3a. The broad nature of the single emission at 56 eV is consistent with Fe(III) occupying a wide range of sites, as expected from the amorphous nature of the walls, which usually leads to a wider dispersion of metal environments as compared to the crystalline phase. The unsymmetrical nature of this emission is due to overlapping 3/2 and 1/2 emissions, as commonly observed in other Fe based materials.[38] Materials synthesized at different metal-to-surfactant ratios displayed virtually identical XPS spectra, as expected given the similar composition.

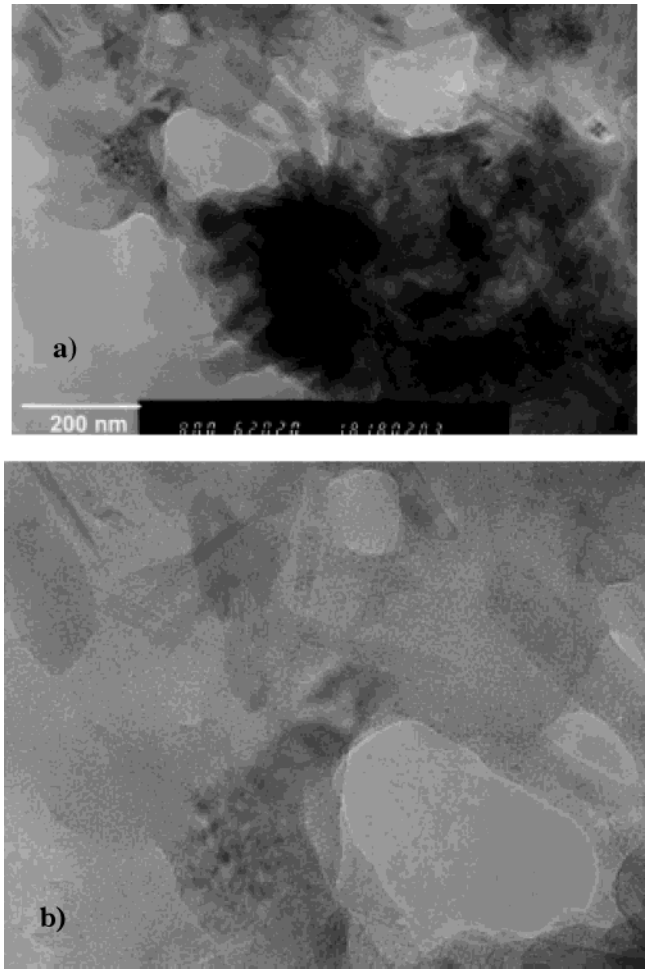

Figure 2. (a) TEM micrograph of mesostructured iron oxide synthesized with a metal-to-surfactant ratio of 3:1; (b) expansion (2×) from (a).

The temperature dependence of the magnetization for the 3:1 material shown in Figure 4a and the magnetic hysteresis curves displayed in Figure 4b are consistent with the presence of at

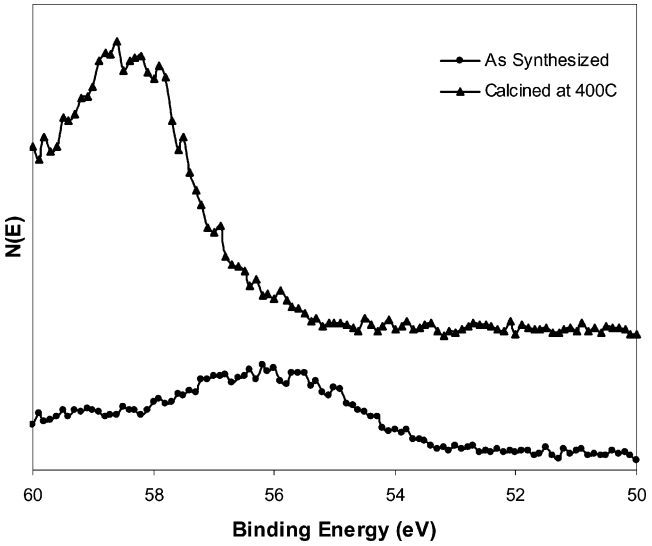

Figure 3. Fe 2p region of the XPS spectra of (a) mesostructured iron oxide synthesized with a 3:1 metal-to-surfactant ratio and (b) of the 3:1 sample after calcination in air for 8 h.

least two magnetic "phases" or behaviors. (i) First, a small, but noticeable bifurcation occurs between the field-cooled (FC) and the zero-field-cooled (ZFC) magnetizations ca. 250 K. This bifurcation typically arises from the presence of a few, very large superparamagnetic particles becoming frozen below 250 K. Most probably, this feature arises from the discrete, rodlike crystals of maghemite (γ-Fe_2O_3) observed in the XRD and TEM studies, as crystals of hematite (α-Fe_2O_3) are only expected to contribute to the magnetic behavior of the composite in a negligible way. The small value of the magnetic remanence at 100 K (1.6×10^{-2} emu/g) would suggest that only 0.02% of the mass of the material would have to be associated with these rodlike γ-Fe_2O_3 crystals to cause this observable effect in the temperature dependence of the magnetization below 250 K. (ii) Although this bifurcation of the ZFC and FC magnetization at 250 K tends to mask any simple Curie-like temperature dependence of the curves below 250 K, the qualitative temperature dependence plus the S-shaped hysteresis at 5 K in Figure 4b is consistent with the superparamagnetic behavior arising from the smaller-sized Fe_2O_3 structures contained within the walls of the mesostructure. Although no peak is observable in the ZFC curve, which one typically associates with the freezing of the superparamagnetic moments, the absence of the ZFC peak would indicate that the majority of these particles/chains are small and able to relax to their equilibrium orientation. For comparison, a peak has been observed below 4 K in mesolammelar iron oxyhydroxides synthesized with alkyl sulfate surfactants.[32] Because the grains in the walls are not expected to be spherical, calculations of the exact superparamagnetic

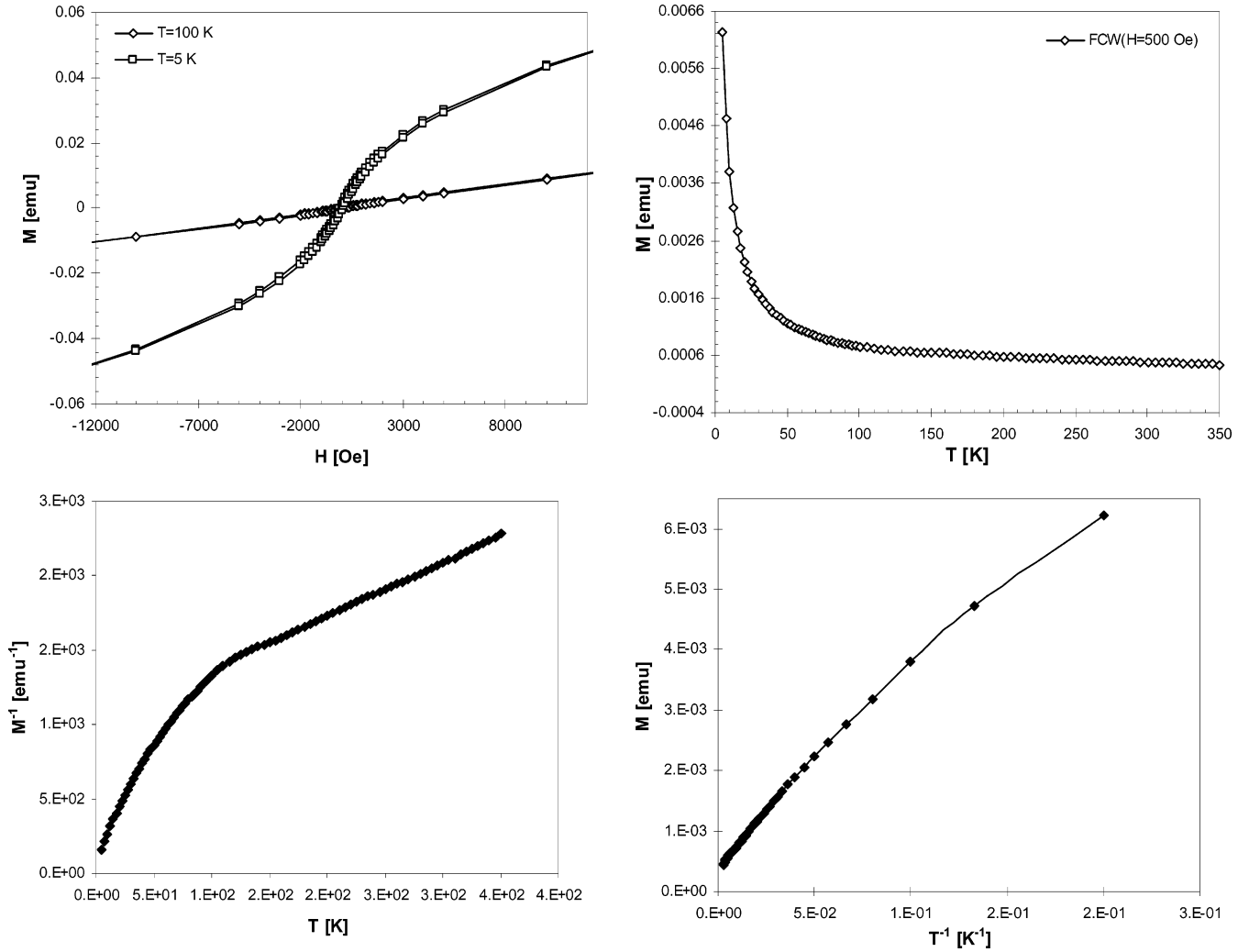

Figure 4. (a) The temperature dependence of the magnetization (M/H) for mesostructured iron oxide synthesized with a metal-to-surfactant ratio of 3:1 and (b) the field dependence at 100 and 5 K. The inset in Figure 4a shows the temperature dependence of the $\Delta M/H$ (=(FCM−ZFCM)/H).

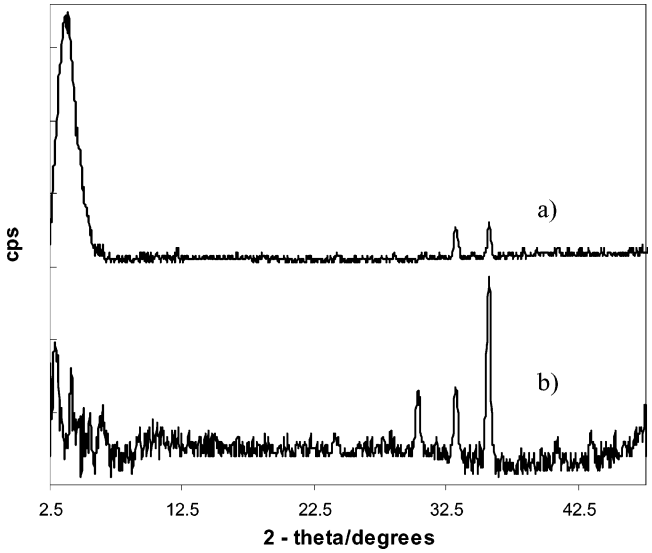

Figure 5. XRD patterns for (a) mesostructured iron oxide synthesized with a metal-to-surfactant ratio of 3:1 and heat treated at 200 °C for 8 h and (b) mesostructured iron oxide synthesized with a metal-to-surfactant ratio of 3:1 after calcination in air at 400 °C for 8 h.

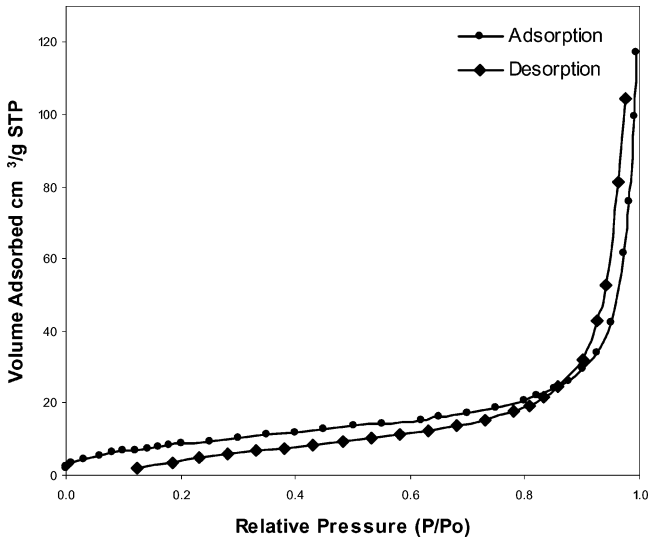

Figure 6. Nitrogen adsorption−desorption isotherm for the 3:1 material after calcination in air at 400 °C for 8 h.

domain size using magnetic anisotropy values in conjunction with the magnetic data above would not yield accurate results.

This interpretation of the magnetic behavior resulting from two magnetic phases is more readily observable in the temperature dependence of the difference between the FC and ZFC magnetizations ($\Delta M/H$), shown in the inset of Figure 4a. One notes a sizable increase in magnitude between 250 and 150 K and another increase below 30 K that continues to increase in magnitude with decreasing temperatures. The increase in the 250−150 K temperature range would be associated with the freezing of the rodlike maghemite crystals, while the increase below 30 K would arise from freezing of the largest Fe_2O_3 particles/chains within the walls.

While amine templates can readily be removed by protonation of the N−M (M = Ta, Ti, Nb) bond in the as-synthesized material, leading to formation of alkylammonium surfactants which can readily be washed out of the structure, this option is not available for the substantially less basic hydroxyl headgroup. Hence, removal of the surfactant was attempted by Soxhlet extraction with ethanol over several days for materials synthesized at all four metal-to-surfactant ratios. This led to little change in the materials and a reduction in C-content of only 2−3%, indicating that the tris-chelating interaction of the

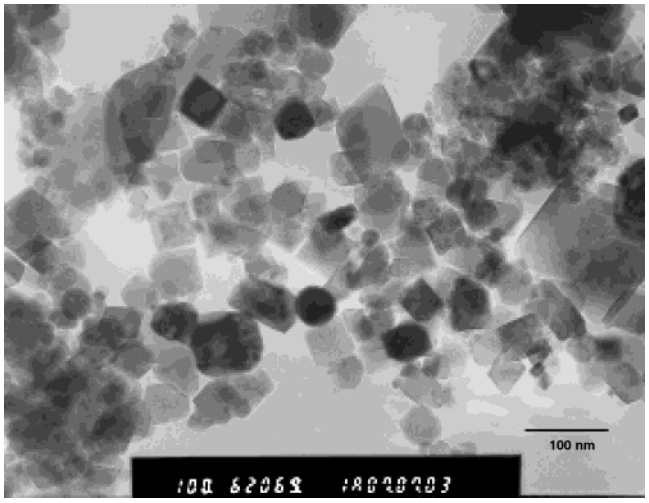

Figure 7. TEM micrograph for the 3:1 material after calcination in air at 400 °C for 8 h.

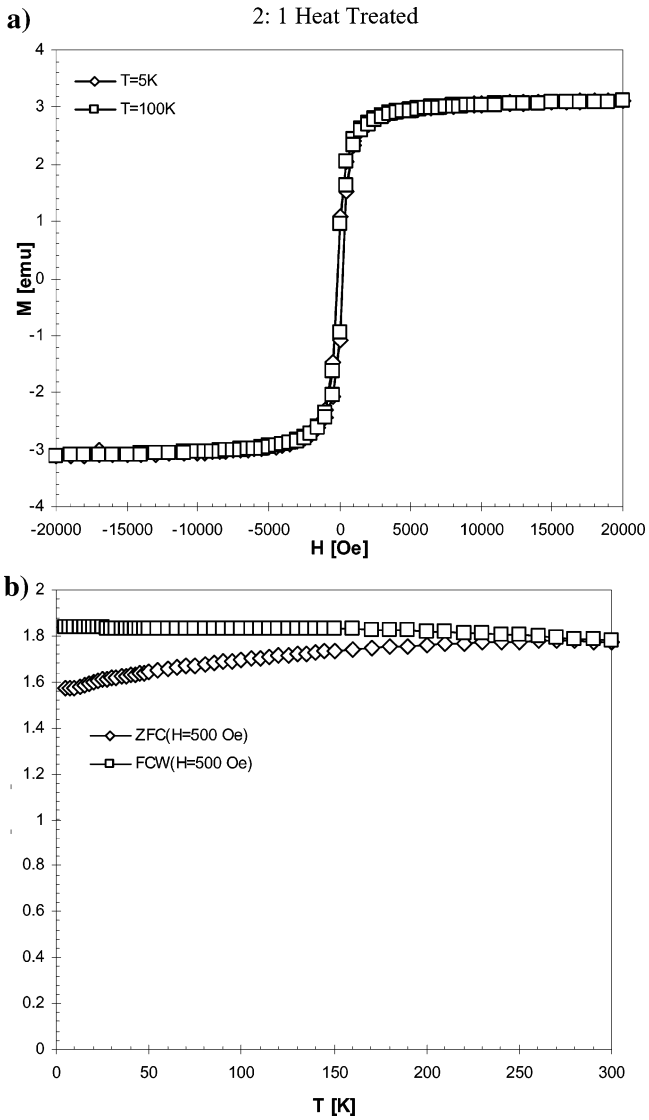

Figure 8. (a) The temperature dependence and (b) field dependence of the magnetization for the 3:1 material after calcination in air at 400 °C for 8 h.

surfactant headgroup is too strong to displace with a monodentate alcohol. Washing in ethylene glycol, a bis-chelating alcohol, also proved unsuccessful in removing the surfactant. Attempts to displace the triol group with ammonium sulfate, ammonium phosphate, or glacial acetic acid led to formation of low surface area amorphous phases with only 30−40% removal of the surfactant. In these experiments, it was envisioned that the sulfate, phosphate, or acetate group would bind preferentially to the Fe centers as compared to the triol; however, whatever surfactant was removed from the structure did not appear to open up any accessible void space, as evidenced by the <5 m^2/g surface areas. Attempts to synthesize Fe oxide mesophases with bis-chelating oxygen surfactants possessing acetylacetone headgroups failed because the surfactant did not remain bound to the inorganic phase during the hydrolysis and subsequent aging steps of the synthesis, although these templates do indeed form discrete complexes with iron ethoxide.[39]

Heat treatment and calcination was attempted as a last means of removing the template. Figure 5 shows an XRD pattern of the 3:1 material after heating at 200 °C for 8 h. The structure is stable under these conditions; however, a loss of the XRD pattern is observed for calcinating temperatures higher than 250 °C. At 400 °C for 8 h, the surfactant can be completely burned out, as evidenced by elemental analysis showing less than 0.1% C. The XRD pattern of this material confirms only the presence of maghemite (Figure 5b) with no evidence of hematite or any retention of the mesostructure. Figure 6 shows the nitrogen adsorption−desorption isotherm of this material. The shape and low adsorption maximum provides further evidence for the loss of the mesostructure. The BET surface area of this material is 32 m^2/g, which is consistent with nanograins possessing limited porosity. The XPS spectrum shows a shift in binding energy to a much narrower emission at 58 eV, consistent with crystallization to a more ordered phase with a narrower distribution of Fe(III) sites. The TEM micrographs for this material, shown in Figure 7, indicate a typical crystal size of 10−50 nm with a small amount of crystallites in the 50−150 nm size range.

The magnetic characteristics for the calcined materials are significantly different from the as-prepared materials. The M/H versus T graph (see Figure 8a) for the 3:1 material calcined at 400 °C shows (i) a bifurcation between the FC and ZFC magnetizations occurring at the highest temperature of 380 K that was measured, (ii) a FC magnetization that becomes saturated for temperatures below 150 K, and (iii) a broad maximum in the ZFC magnetization centered at around 280 K. Although these features are also consistent with superparamagnetic behavior for a wide distribution of very large particle sizes, this description may be less appropriate as the TEM micrographs indicate ferromagnetic crystals of 10−50 nm in size, which would behave more like bulk Fe_2O_3 with multidomain structures. The magnetic hysteresis curves in Figure 8b are also consistent with the material being described as a soft ferromagnet material with small hysteretic behavior (remanence of 14 emu/g and coercivity of 190 Oe). The saturation magnetization value of 47 emu/g would suggest that 56% of the material is maghemite ($M_{sat} = 83.7$ emu/g).

Conclusion

Mesostructured iron oxide was synthesized with a tris-chelating triol surfactant. While this material is unique in that it represents the first mesostructured iron material without sulfate or phosphate that possesses an XRD peak assignable to the repeat distance of the mesostructure, the surfactant cannot be removed without collapse of the structure and formation of 10−50 nm crystallites of a dense iron oxide phase exhibiting soft ferromagnetic properties. The as-synthesized mesostructure displays a superparamagnetic behavior, which indicates that iron oxide nanoparticles/structures are formed in the walls. The results in this study indicate that other chelating oxygen surfactants may yet be successful in synthesizing stable mesoporous iron oxide with surface areas comparable or higher than other samples of mesoporous iron oxide previously synthesized

Acknowledgment. The authors would like to acknowledge Natural Sciences Engineering Research Council (NSERC) and the Petroleum Research Fund (PRF) administered by the American Chemical Society.

References and Notes

(1) Kresge, C. T.; Leonowicz, M. E.; Roth, W. J.; Vartulli, J. C.; Beck, J. S. *Nature* **1992**, *359*, 710.
(2) Beck, J. S.; Vartuli, J. C.; Roth, W. J.; Leonowicz, M. E.; Kresge, C. T.; Schmitt, K. D.; Chu, C. T.-W.; Olson, D. H.; Shepard, E. W.; McCullen, S. B.; Higgins, J. B.; Schlenker, J. L. J. *Am. Chem. Soc.* **1992**,*114*, 10834.
(3) Monnier, A.; Schuth, F.; Huo, Q.; Kumar, D.; Margolese, D.; Maxwell, R. S.; Stucky, G. D.; Krishnamurty, M.; Petroff, P.; Firouzi, A.; Janicke, M.; Chmelka, B. F. *Science* **1993**, *261*, 3.
(4) Huo, Q.; Margolese, D. I.; Cielsa, U.; Feng, P.; Gier, T. E.; Sieger, P.; Leon, R.; Petroff, P. M.; Schuth, F.; Stucky, G. *Nature* **1994**, *368*, 317.
(5) Davis, M. E. *Nature* **1993**, *364*, 391.
(6) Antonelli, D. M.; Ying, J. Y. *Cur. Opin. Coll. Interface Sci*. **1996**, *1*, 523.
(7) Imhof, A.; Pine, D. J. *Nature* **1997**, *389*, 948.
(8) Mann, S. *Nature* **1993**, *365*, 499.
(9) Mann, S.; Ozin, G. A. *Nature* **1996**, *382*, 313.
(10) Huo, Q.; Leon, R.; Petroff, P. M.; Stucky, G. D. *Science* **1995**, *268*, 1324.
(11) Tanev, P. T.; Chibwe, M.; Pinnavaia, T. J. *Nature* **1997**, *368*, 321.
(12) Stein, A. *Adv. Mater*. **2003**, *15*, 763.
(13) Ying, J. Y.; Mehnert, C. P.; Wong, M. S. *Angew. Chem., Int. Ed.* **1999**, *38*, 56.
(14) Keefe, M. H.; Slone, R. V.; Hupp, J. T. Czaplewski, K. F.; Snurr, R. Q.; Stem, C. L. *Langmuir* **2000**, *39*, 19.
(15) Morris, C. A.; Anderson, M. L.; Stroud, R. M.; Merzbacher, C. I.; Rolison, D. R. *Science* **1999**, *284*, 622.
(16) Gratzel, M. *Curr. Opin. Colloid Sci*. **1999**, *4*, 314.
(17) MacLachlan, M. J.; Ginzburg. M.; Coombs, N.; Raju, N. P.; Greedan, J. E.; Ozin, G. A.; Manners, I. *J. Am. Chem. Soc.* **2000**, *122*, 3878.
(18) Ingaki, S.; Guan, S.; Fukushima, Y.; Oshuna, T.; Terasaki, O. *J. Am. Chem. Soc*. **1999**, *121*, 9611.
(19) Melde, B. J.; Holland, B. T.; Blanford, C. F.; Stein, A. *Chem. Mater*. **1999**, *11*, 3302.
(20) Asefa, T.; MacLachlan, M. J.; Coombs, N.; Ozin, G. A. *Nature* **1999**, *402*, 867.
(21) Antonelli, D. M.; Ying, J. Y. *Angew. Chem. Int. Ed. Engl*. **1995**, *34*, 2014.
(22) Antonelli, D. M.; Ying, J. Y. *Angew. Chem., Int. Ed. Engl*. **1995**, *35*, 426.
(23) Tian, Z.-R.; Tong, W.; Wang, J.-Y.; Duan, N.-G.; Krishnan, V. V.; Suib, S. L. *Science* **1997**, *276*, 926.
(24) Antonelli, D. M.; Trudeau, M. *Angew. Chem., Int. Ed.* **1999**, *38*, 1471.
(25) He, X.; Antonelli, D. M. *Angew. Chem., Int. Ed.* **2002**, *41*, 214.
(26) Reddy, J. S.; Sayari, A. *Catal. Lett.* **1996**, *38*, 219.
(27) Ciesla, U.; Schacht, S.; Stucky, G. D.; Unger, K.; Schuth, F. *Angew. Chem., Int. Ed. Engl.* **1996**, *35*, 541.
(28) Rangan, K. K.; Billinge, S. J. L.; Petkov, V.; Heising, J.; Kanatzidis, M. G. *Chem. Mater*. **1999**, *11*, 2629.
(29) MacLachlan, M. J.; Coombs, N.; Ozin, G. A. *Nature* **1999**, *397*, 681.
(30) Braun, P. V.; Osenar, P.; Stupp, S. I. *Nature* **1996**, *380*, 325.
(31) Guo, X.; Ding, W.; Wang, X.; Yan, Q. *Chem. Commun*. **2001**, 709.
(32) Tolbert, S. H.; Sieger, P.; Stucky, G. D.; Aubin, S. M. J.; Wu, C.-C.; Hendrickson, D. N. *J. Am. Chem. Soc*. **1997**, *119*, 8652.
(33) Wirnsberger, G.; Gatterer, K.; Fritzer, H. P.; Grogger, W.; Pillep, B.; Behrens, P.; Hansen, M. F.; Bender Koch, C. *Chem. Mater*. **2001**, *13*, 1453.
(34) Srivastava, D. N.; Perkas, N.; Gedanken, A.; Felner, I. *J. Phys. Chem. B* **2002**, *106*, 1878.
(35) Antonelli, D. M. *Microporous Mesoporous Mater*. **1999**, *28*, 505.
(36) Weibel, B.; Matell, M. *Acta Chem. Scand*. **1962**, *16*, 1062.

(37) Formation of micellar aggregates in solution is rationalized in terms of the relative balance between several offsetting parameters. The ensemble of these parameters can be described in terms of the effective surfactant packing parameter $g = V/a_o l$, where V is the total volume of the surfactant chains, a_o is the effective headgroup area at the micelle surface, and l is the kinetic surfactant chain length. Spherical micelles will form if $g < 1/3$, rodlike micelles will form if $1/3 < g < 1/2$, vessicles or bilayers if $1/2 < g < 1$, and inverted micelles if $g > 1$. Solution conditions can dramatically alter the micellar array formed so that by adding inorganics to a solution containing spherical micelles, rodlike organic−inorganic composites can form.

(38) Antonelli, D. M. *Adv. Mater.* **1999**, *11*, 488.

(39) Tamura, E.; Waddill, G. D.; Tobin, J. G.; Sterne, P. A. *Phys. Rev. Lett.* **1994**, *73*, 1533.

(40) Lezau, A.; Antonelli, D. M. Unpublished results.